***PREPRINT**: Blocken B, Carmeliet J. 2006. On the accuracy of wind-driven rain measurements on buildings. Building and Environment 41(12): 1798-1810. © Elsevier 2006.*

On the accuracy of wind-driven rain measurements on buildings

Bert Blocken [a*], Jan Carmeliet [a,b]

[a]*Laboratory of Building Physics, Department of Civil Engineering, Katholieke Universiteit Leuven, Kasteelpark Arenberg 40, 3001 Leuven, Belgium*
[b]*Building Physics Group, Faculty of Building and Architecture, Technical University Eindhoven, P.O. box 513, 5600 MB Eindhoven, The Netherlands*

Abstract

Wind-driven rain (WDR) measurements on buildings are being conducted for many decades. They provide an indication of the WDR falling onto different parts of a building facade and are an essential tool for WDR model development and model validation. However, up to now, very few investigations concerning the accuracy of WDR measurements have been performed. No publication of WDR measurements has been found that provides an indication of the errors involved. Availability of error estimates is essential for the interpretation and the use of WDR measurement data. In this paper, the main errors associated with WDR measurements are identified and investigated. It is shown that especially the evaporation of adhesion water from the gauge catch area can be important and a method to estimate this error will be proposed. It is shown that this error can be very large (up to 100%) and that it depends not only on the gauge type but also on the type of rain event. Finally, guidelines for the design of WDR gauges and for the selection of WDR measurement data that are suitable for model development and model validation are given.

Keywords: Wind-driven rain; Driving rain; Wind flow; Building facade; Experimental; Accuracy; Error; Evaporation; Runoff; Splashing

1. Introduction

Wind-driven rain (WDR) is one of the most important moisture sources affecting the hygrothermal performance and the durability of building facades. Information concerning the exposure to WDR is essential to design building facades with a satisfactory hygrothermal performance. Knowledge on the quantity of WDR is also an essential requirement as a boundary condition for Heat-Air-Moisture (HAM) transfer analysis. Different methods exist for quantifying the WDR amount that falls onto building facades: measurements, semi-empirical formulae and numerical simulations based on Computational Fluid Dynamics (CFD). A review of these methods was given by Blocken and Carmeliet [1].

For many decades, measurements have been the primary tool in WDR research. Although semi-empirical models and numerical simulation models are increasingly being used for quantifying WDR, measurements remain important as they are the essential basis for model development and model validation. For example, the vast increase of the use of CFD in WDR studies, as reported in [1] (e.g. [2-7]) and the subsequent need for CFD validation have exposed the lack of reliable and complete WDR measurement data on different building configurations. As a result, much experimental work will be needed in the future, and conducting WDR measurements will remain at least as important as it has been during the past decades.

Measurements of WDR on buildings are performed with WDR gauges. These gauges are all of a similar basic design (Fig. 1). They consist of a collection plate, a draining tube and a reservoir. The

* Corresponding author: Bert Blocken, Laboratory of Building Physics, K.U.Leuven, Kasteelpark Arenberg 40, B-3001 Leuven, Belgium. Tel.: +32 (0) 16-321345 - Fax: +32 (0) 16-321980
E-mail address: bert.blocken@bwk.kuleuven.be

collection area is made up of a shallow tray (collection area or catch area) of some material, shape and size and it is fixed at the building surface. It has a raised rim around the perimeter to prevent the collection of water from outside the collection area. The volume or weight of the collected rainwater in the reservoir is manually or automatically registered at regular intervals.

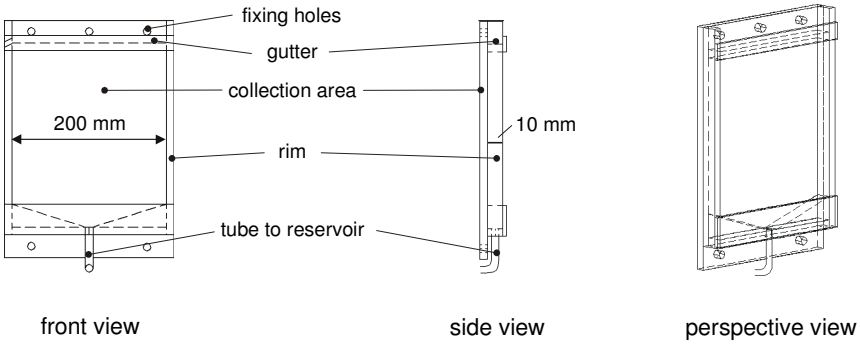

Fig. 1. Wind-driven rain gauge designed, manufactured and installed at the Laboratory of Building Physics, K.U.Leuven. The gauge is made of PMMA (polymethyl-methacrylate) with a collection area A = 0.2x0.2 m².

WDR gauges are not industrially manufactured and there exists no standard on their design. As a result, there are almost as many types of WDR gauges as there are researchers using them. Although the basic design is the same, these gauges differ by material, shape and size of the collection area, the draining tube and the reservoir. In the past, a few comparative studies of the performance of different WDR gauges were undertaken. In 1964 and 1965, Hendry [8] and Lacy [9] found some occasional discrepancies but no large differences on the whole. In 1977, Meert and Van Ackere [10] indicated the form of the gauge to have some influence. In 1999, Högberg et al. [11] reported differences of 100% in WDR catch by different gauges that were placed next to each other on a building facade for a 5-month period. Up to now, no detailed investigation concerning the errors associated with different WDR gauges has been performed. Many questions have been raised that remain unanswered. It is not clear why the readings by different gauges can differ that much and what are the important parameters governing gauge accuracy and gauge performance. Furthermore, there is no method available to estimate the error associated with WDR measurements.

The intention of this paper is (1) to identify the possible error sources; (2) to explain why WDR measurement errors can be that important; (3) to provide a way to estimate the possible adhesion-water-evaporation error for a given WDR gauge and a given rain event; (4) to indicate the importance of the other errors associated with WDR measurements and (5) to provide guidelines for the design of WDR gauges and for the selection of accurate WDR measurement data. In section 2, the error sources are identified and the recent comparative study reported by Högberg et al. [11] is briefly outlined and discussed, because of its importance for the present study. In section 3, the adhesion-water-evaporation error is studied and the reason for the differences observed by Högberg et al. [11] is given. Section 4 focuses on the importance of the other error sources. In section 5 and 6, guidelines for gauge design and data selection are given. In section 7, some measurement results and their error estimates are presented. Section 8 and section 9 respectively comprise the discussion and the conclusions.

2. Literature review: comparative study of wind-driven rain gauges

The possible errors associated with WDR measurements are: (1) evaporation of adhesion water from the collection area (and from the inner side of the draining tube), (2) evaporative losses from the reservoir, (3) splashing of drops from the collection area, (4) condensation on the collection area and (5) wind errors.

A brief literature review is presented concerning the gauge-comparative study that was conducted by van Mook, Högberg and Kragh [11]. The comparative study was a joint research project of the Building

Physics groups of the Technical University of Eindhoven (TUE), Chalmers University of Technology (CTH) and the Technical University of Denmark (TUD). This experimental study included, for the first time, gauges that were specifically designed to measure adhesion water. During and after a WDR event, there is always an amount of water (individual drops or water film) adhered to the collection area. This amount is not collected in the reservoir and hence not measured. After and to a lesser extent also during rain, this *adhesion water* evaporates. Kragh [12] at the TUD developed a WDR gauge that deviates from traditional gauges in that it is suspended from a load cell, allowing both the collected amount of WDR in the reservoir and the amount of drops adhered to the gauge surface to be registered (Fig. 2). Van Mook [13,14] at the TUE designed a WDR gauge that is equipped with an automated wiper to collect the adhesion water from the collection area (Fig. 3). The comparative study conducted by the three universities and reported by Högberg et al. [11] included these two special WDR gauges together with two traditional WDR gauges (i.e. without specific features to measure adhesion water). The gauges can be described as follows:

1. A traditional WDR gauge with a collection plate made of PMMA (polymethyl-methacrylate) and with a small, square catch area A = 0.032 m². It is called "CTH" after the name of the university where it was developed.
2. A traditional WDR gauge with a collection plate covered with PTFE (polytetra-fluoroethylene) and with a large, circular catch area A = 0.44 m². This gauge is almost identical to the one illustrated in Fig. 3, but without wiper. It is called "TUE-I".
3. The special WDR gauge with wiper, with a collection plate covered with PTFE and with a large, circular catch area A = 0.50 m² (Fig. 3). It is called "TUE-II".
4. The special load-cell-suspended WDR gauge (Fig. 2) with a collection plate made of stainless steel and with a rectangular catch area A = 0.21 m², called "TUD".

The PTFE surface finish of the gauges TUE-I and TUE-II was chosen because of its hydrophobic character. It was expected that this would improve the runoff of drops from the collection area to the reservoir and hence reduce the amount of adhesion water. The four gauges were positioned side-by-side on the west facade of a high-rise building (the main building of the TUE) and were exposed to WDR for five months (Fig. 4).

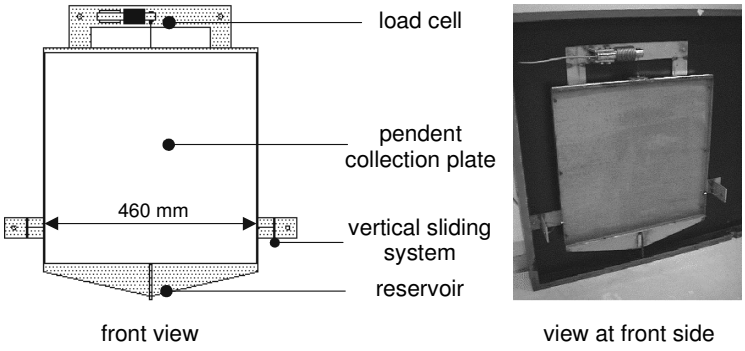

Fig. 2. Special wind-driven rain gauge designed to measure adhesion water. The collection plate and the reservoir are suspended from a load cell (figure partly from [5], ©van Mook 2003, reproduced with permission).

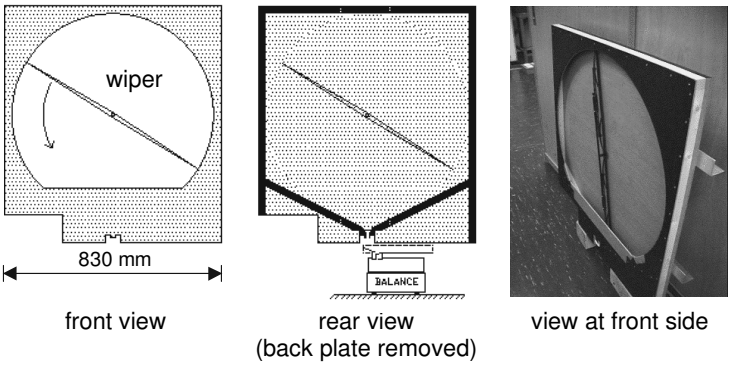

Fig. 3. Special wind-driven rain gauge designed to measure adhesion water. The collection area is equipped with an automated wiper (figure partly from [5], ©van Mook 2003, reproduced with permission).

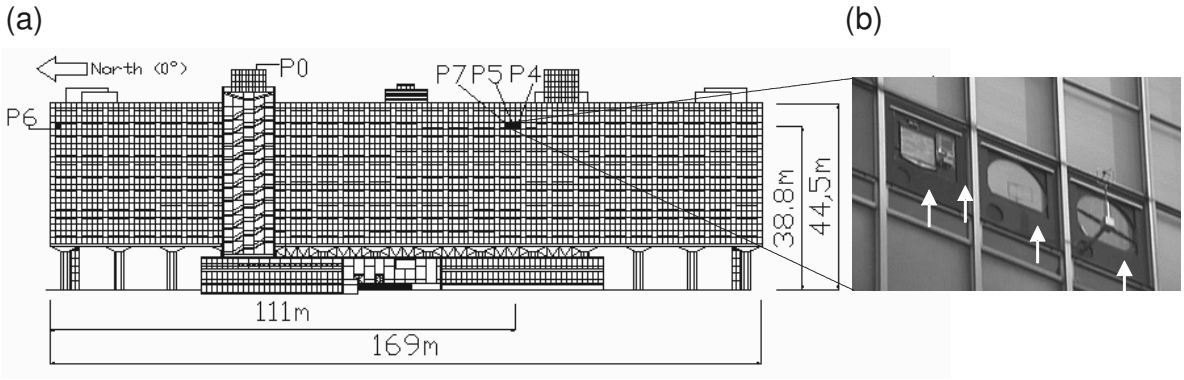

Fig. 4. Measurement set-up for the comparative test of wind-driven rain gauges. (a) The west facade of the TUE main building. The positions of the wind-driven rain gauges that are involved in the test are indicated by the labels “P7”, ”P5”, “P4”. (b) Wind-driven rain gauges exposed next to each other. From left to right: the TUD gauge, the CTH gauge, the TUE-I gauge and the TUE-II gauge (figure partly from [5], ©van Mook 2004, reproduced with permission).

The results were rather remarkable. At the end of the 5-month period it was found that [11]:

1. The CTH gauge (no wiper) and the TUE-II gauge (with wiper) had caught about the same amount of WDR (about 22 mm).
2. The TUD gauge had caught slightly more WDR (24 mm) than CTH and TUE-II.
3. The TUE-I gauge had caught less than half the amount that had been measured by the other gauges (only 10 mm!)

Högberg et al. [11] concluded that:

1. Given the difference between the TUE-I and the TUE-II gauges, a wiper is a necessary feature for large collection areas.
2. Given the bad result by the TUE-I gauge, a PTFE surface finish is not a sufficient measure.

The first conclusion implies that adhesion-water evaporation is an important error source on PTFE surfaces. As the gauges TUE-I and TUE-II were exposed next to each other and were similar (apart from the wiper aspect), all other errors will have acted in the same way on both gauges. Therefore we have to conclude that adhesion-water evaporation is the only reason for the different performance of these two gauges. This error does not appear to be very important for the small PMMA surface (given the good performance of the CTH gauge). The reason for the large differences between the readings of the gauges TUE-I and TUE-II will be studied and explained in more detail in the next section.

3. Study of the adhesion-water-evaporation error

In this section, the focus is on the adhesion-water-evaporation error, as it is considered to be very important according to the comparative study reported in section 2. The other errors will be addressed in section 4.

3.1. Adhesion of water on a vertical surface

To gain some insight into the mechanisms involved in the build-up of an amount of adhesion water on a vertical surface (gauge collection area), a simplified numerical study and a number of experiments have been conducted.

3.1.1. Numerical study of water adhesion on a vertical surface

The numerical study comprises the simplified simulation of the behaviour of raindrops after impact on a vertical, impervious, smooth surface (collection area). It consists of dividing the collection area into a large number of small square areas and of running a Monte-Carlo simulation by which raindrops of a given size are attached to a certain position (square area) of the collection area (no splashing assumed) (Fig. 5). A raindrop of diameter d reaching the vertical collection area spreads out to form a "surface-pendent drop" with a certain base diameter d_{SPD}. As the simulation proceeds, the collection area is "wetted" by a scatter of raindrops. When a raindrop is attached to a square area on which there is already another drop, the drops coagulate and the volumes of both drops are added. When the added volume exceeds a limit value, the drop runs down the collection area, rinsing it partly and taking all drops that it finds on its way down with it. By doing this, a small trace of tiny droplet fragments (trace droplets) is left behind. The volume of water that has run down is then added to the reservoir and is denoted "the collected or measured WDR". All other drops that are adhered to the collection area are called "adhesion water" (Fig. 5). The total volume of raindrops that has been assigned to parts of the collection area since the start of the simulation is called "the inflicted WDR". To be able to perform simulations, a number of parameters have to be (empirically) determined and set in the program code: (1) the size of the square areas ($A_{AREA} = s_{AREA}^2$), (2) the diameter of the impacting drops (d), (3) the limit base diameter or volume for runoff (d_{LIMIT} or V_{LIMIT}), (4) the relation between the limit base diameter d_{LIMIT} of the surface-pendent drop and the limit surface-pendent-drop volume V_{LIMIT}, (5) the base diameter of the trace droplets (d_{TRACE}), (6) the spacing between the trace droplets (s_{TRACE}) and (7) the relation between d_{TRACE} and the corresponding volume V_{TRACE}. Fig. 5 is a schematic representation of this numerical model. It shows the vertical collection area of the gauge, which is covered with a number of surface-pendent drops (adhesion water). One of the drops has reached the limit base diameter d_{LIMIT} and runs of from the collection area, leaving some trace droplets behind on its way down. When this drop reaches the bottom part of the collection area, its remaining volume is added to the reservoir.

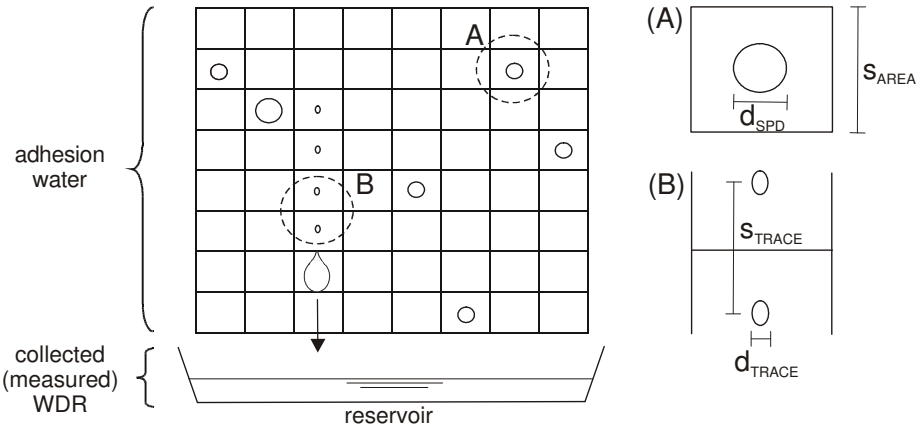

Fig. 5. Schematic representation of the numerical model for raindrop adhesion, coagulation and runoff on a vertical surface. (A) and (B) are detail figures of a surface-pendent drop and of two trace droplets, respectively.

The idea of simulating the adhesion, coagulation and runoff of drops on a vertical surface originated from a large number of experimental observations. Simplified tests were conducted in which water droplets were sprayed on a clean vertical PMMA surface using a plant-sprayer with an adjustable nozzle. The following observations were made: (1) The limit base diameter of a drop for runoff (d_{LIMIT}) is fairly constant (4-5 mm). (2) When runoff occurs, the drop follows a fairly straight path down, taking all drops on its path with it and leaving a trace of small drops behind. (3) The base diameter d_{TRACE} (1 mm) and the (vertical) spacing between the trace droplets (s_{TRACE} = 8 to 10 mm) are remarkably fixed. These values were used for the parameters in the numerical model. Additionally, the following settings were selected: (1) A_{AREA} = 5x5 mm², based on the value of d_{LIMIT}; (2) all drops falling on the surface have the same diameter d = 1 mm; (3) the relation between the limit base diameter d_{LIMIT} for runoff and the corresponding limit volume V_{LIMIT} is given by $V_{LIMIT} = \pi(d_{LIMIT})^3/18$ (i.e., 1/3 of a sphere); (4) The relationship between the trace-droplet diameter d_{TRACE} and the trace-droplet volume V_{TRACE} is given by $V_{TRACE} = \pi(d_{TRACE})^3/12$ (i.e., 1/2 of a sphere). The latter two relationships are based on visual observations of the limit and trace drops. It is noted that they are only estimates and not measurement results.

Fig. 6 illustrates the results of a simulation run with these settings for a vertical rectangular PMMA plate representing a collection area A = 0.45x0.25 m². The straight line is the cumulative inflicted WDR. It is the sum of the adhesion water and the collected or measured WDR. The main observation from this graph is the existence of two stages: (1) for a cumulative inflicted amount of WDR smaller than about 0.12 mm (threshold value), all water is adhered to the collection area and no WDR is measured; (2) Above this threshold value, the volume of adhesion water (in L/m² or mm) decreases to a value that fluctuates between an upper and a lower boundary (0.05 and 0.08 mm). Although this numerical study is based on a number of assumptions and although the calibration was only made for one specific surface material (PMMA) and one nozzle setting, it serves the purpose of illustrating the mechanism by which a volume of adhesion water builds up and remains on the collection area.

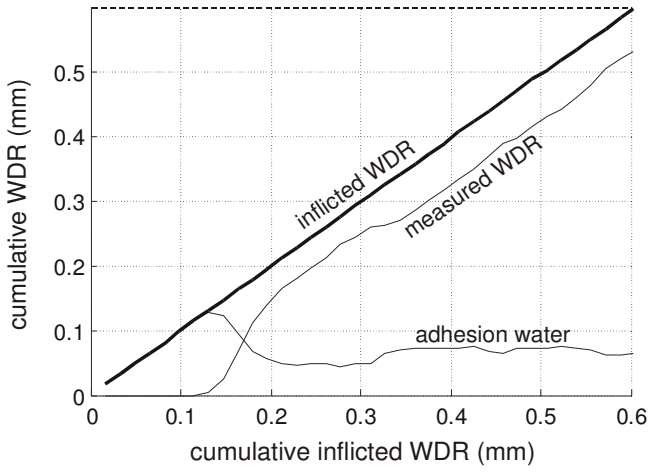

Fig. 6. Result of the numerical simulation of drop adhesion, coagulation and runoff on an impervious, smooth, vertical PMMA surface. The “cumulative inflicted WDR” is the total amount of rainwater impinging on the surface. The “measured WDR” is the amount that has run off into the reservoir. The curve “adhesion water” indicates the amount of water that is adhered to the surface.

3.1.2. Experimental study of water adhesion on a vertical surface

To determine the quantity of adhesion water that can be present at vertical surfaces of different materials, experimental studies similar to the one mentioned in the previous section were conducted for rectangular plates made out of (1) PVC; (2) PMMA; (3) PTFE; (4) ordinary sheet glass; (5) glass with a hydrophilic coating and (6) glass with a hydrophobic coating. Each plate was subjected to 30 spraying cycles. In each cycle, spraying went on until a significant amount of runoff (i.e. water in the reservoir) was collected. Note that this way, the nozzle setting (impinging raindrop diameter) is eliminated as a parameter, as many drops are needed at approximately the same position at the surface before runoff

occurs. This statement was verified by conducting the same experiments with other nozzle settings, which yielded very similar results. After each cycle, the plate was weighed and the mass of the adhesion water registered. Tap water was used for these experiments. One could argue that the amount of adhesion water on a vertical surface might be related to the contact angle of a water drop on that surface. Therefore, contact angles for each of the six materials were measured using a drop-shape-analysis system employing the optical sessile-drop method. It consists of placing tiny droplets (volume of 1 µL) on a horizontal material surface and determining the contact angle from a photovisual image. Fig. 7 shows two of these images, for sessile drops on a PVC surface and on an ordinary-sheet-glass surface. Table 1 summarises the results of the contact-angle and adhesion-water measurements. For the latter, both the average value and the standard deviation are given. These values were obtained by dividing the volume of adhesion water by the area of the plate. The units are L/m² (= mm). The following observations are made:

1. The contact angles of PVC, PMMA and PTFE show little difference. As they are larger than 90°, all three materials are called *hydrophobic*. Despite their similar contact angles, the amount of adhesion water differs considerably.
2. The glass plates (Glass1 and 2) are hydrophilic. They have a different contact angle but the same small amount of adhesion water.
3. PTFE and Glass3 (with hydrophobic coating) hold the largest amount of adhesion water.

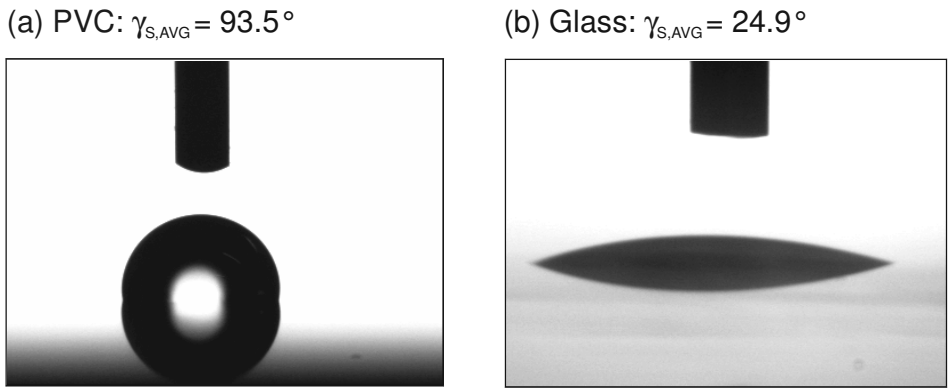

Fig. 7. Photovisual images of sessile water droplets (volume of 1µL) on a horizontal material surface for contact-angle measurements with the optical sessile-drop method. (a) Droplet on a PVC surface with an average contact angle $\gamma_{S,AVG}$ = 93.5°. (b) Droplet on an ordinary-sheet-glass surface with an average contact angle $\gamma_{S,AVG}$ = 24.9°.

It is concluded that:

1. The contact-angle measurements do not provide a direct indication of the amount of adhesion water on a vertical surface. This is most likely due to a number of reasons, including (1) the fact that the shape of an individual drop on a horizontal surface is very different from that on a vertical surface (Fig. 8) and (2) the fact that in reality, not all adhesion water is present as individual droplets at the surface, but that droplet coagulation is an important process in the build-up of adhesion water.
2. PTFE, which has been used in WDR measurements in the past because of its “hydrophobic” character, holds the largest amount of adhesion water. It is a known fact that hydrophobic horizontal surfaces hold more water than hydrophilic horizontal surfaces. For vertical surfaces however, the opposite has often been assumed: hydrophobic surfaces have been expected to promote drop run-off. This assumption appears to be incorrect.
3. PMMA, PVC and especially Glass1 and Glass2 hold (much) less adhesion water and the latter should preferably be used for the collection area of WDR gauges.

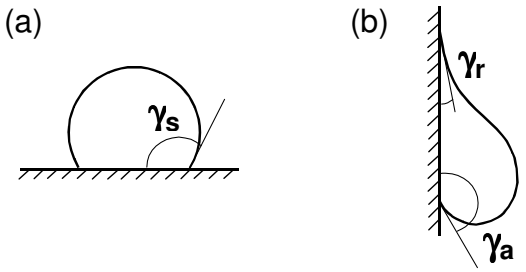

Fig. 8. (a) Contact angle of a sessile drop on a horizontal surface (γ_s). (b) Contact angles of a surface-pendent drop on a vertical surface: advancing (γ_a) and receding (γ_r) contact angles.

3.2. Estimating the error due to evaporation of adhesion water

The adhesion-water-evaporation error can be estimated by assuming no evaporation during rain and total evaporation of the adhesion water when it stops raining. In this case, referring to Fig. 6, the curve "adhesion water" is a measure for the adhesion-water-evaporation error E_{AW} at different impinged cumulative WDR amounts S_{wdr}. When S_{wdr} is below the threshold value, all WDR evaporates and the relative measurement error $e_{AW} = E_{AW}/S_{wdr}$ is 100%. Above the threshold value, the absolute measurement error E_{AW} is approximately constant (see standard deviation in Table 1) and equal to the amount of adhesion water. It is given by the value in Table 1 (AW avg) for the materials tested. The relative measurement error e_{AW} hence decreases as the collected amount of WDR during the rain event increases.

3.3. The importance of the adhesion-water evaporation error

The adhesion-water volumes listed in Table 1 appear small. To understand their importance, information on the impinging WDR intensity and on the duration of WDR is needed. Useful information on this matter for one location, Eindhoven, The Netherlands, has been provided by van Mook [5]. He measured horizontal rainfall intensities R_h (i.e. the rainfall intensity falling through a horizontal plane, as measured by a traditional rain gauge) and WDR intensities R_{wdr} on the west facade of the high-rise TUE main building during a 2-year period (Fig. 4). The WDR measurements used in this paper were made with the accurate TUE-II gauge (see Fig. 3; with wiper and thus with a small AW error) at the position labelled "P7P5/P4" in Fig. 4. We extract the following information from his work:

1. At this position on the facade and for 56% of the total time that WDR is registered, the WDR intensity R_{wdr} is below 0.15 mm/h. For 78% of the time, R_{wdr} is below 0.40 mm/h.
2. 75% of all horizontal-rain periods (with or without WDR) are shorter than 1 hour.

Assuming similarly that 75% of all WDR periods are shorter than 1 hour, it can be assumed that:

1. For 42% of the time with WDR, the cumulative WDR amount S_{wdr} that has impinged on the gauge is less than 0.15 mm.
2. For 59% of the time with WDR, S_{wdr} is less than 0.40 mm.

Combining this information with the AW evaporation errors for PTFE given in Table 1 and assuming total AW evaporation after each WDR period, it is seen that:

1. For 42% of the time with WDR, the error e_{AW} is between 67 and 100%.
2. For 59% of the time with WDR, e_{AW} is between 25 and 100%.

This indicates that AW evaporation can have a very large effect on the amount of WDR measured by a PTFE gauge that is not equipped with a wiper.

Note that the measurements used above were collected at exactly the same location as that where the comparative study between the WDR gauges (including TUE-I without wiper and TUE-II with wiper) was carried out (Fig. 4). The percentages mentioned above confirm that the large difference between the readings of these two gauges can be attributed to AW evaporation.

The simulations and the experiments in subsection 3.1 were performed for rectangular plates representing the gauge collection area. It is expected that for a real WDR gauge with additional details (rim, horizontal part at bottom of gauge with tailpiece that is to be connected to the draining tube, draining tube itself), more adhesion water will be present and that therefore, the error percentages mentioned above will in reality be larger. To confirm this expectation, the possible AW-evaporation error associated with the PVC and PMMA gauges designed and manufactured by the Laboratory of Building

Physics was assessed. The gauges themselves (not only the vertical plates, but the complete gauge assembly, including the rim and copper tailpiece, however without the draining tube) were subjected to 30 spraying cycles. The results given in Table 2 indicate that the amount of adhesion water increases and that the design of the PVC gauge is better than that of the PMMA gauge (Fig. 1). The PMMA gauge holds quite some adhesion water at the bottom of the gauge, on the small horizontal surface near the copper tailpiece. Note that this is the case for the gauges by the Laboratory of Building Physics and that it is not necessarily the case for the gauges used in the comparative study by Högberg et al. [11].

4. Other errors

The errors associated with WDR measurements were listed in the beginning of section 2: (1) AW evaporation; (2) evaporation from the reservoir; (3) drop splashing; (4) condensation on the collection area and (5) wind errors.

The evaporation error from the reservoirs can be measured and the WDR measurements can be corrected for this. For example, for the measurements conducted at the VLIET building of the Laboratory of Building Physics, where the draining tube is led through the facade and where the reservoirs are positioned inside, this error is approximately constant: i.e. about 0.05 mm per day.

Splashing refers to the collision of a water drop on a solid surface. This phenomenon is extremely complex and many factors are involved. Most research in this field has been concerned with the impact of vertically falling drops on horizontal or inclined surfaces. Research of splashing on vertical surfaces has to our knowledge only been reported by Couper in 1974 [15] and by Högberg starting from 1998 [16-18]. Högberg at CTH developed a WDR gauge with a deeply recessed collection area composed of tilted surfaces to avoid splashing losses (Fig. 9). It was found that the performance of this gauge was better than that of non-recessed gauges for high wind speed and heavy rainfall intensities (with large raindrops); whereas the large collection area increased the AW-evaporative losses that dominated performance for light to moderate rainfall intensities. It is indeed logical that splashing becomes more important as the

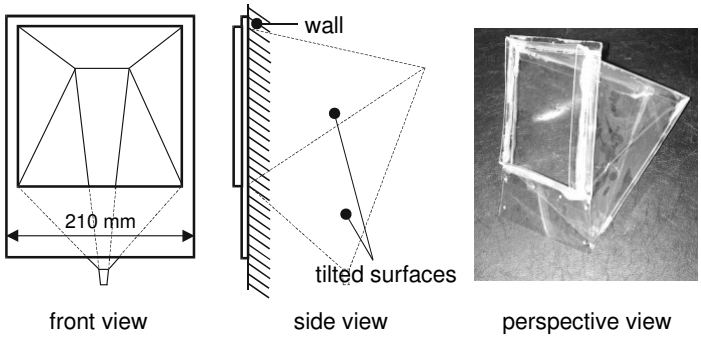

Fig. 9. Special wind-driven rain gauge designed to limit splashing losses [18]. The collection area is deeply recessed and is composed of tilted surfaces.

raindrop size, the raindrop speed and hence the raindrop kinetic energy increase. In wind-tunnel tests of the performance of WDR gauges positioned on a full-scale low-rise building model, where a traditional gauge and the special gauge by Högberg were compared at high WDR intensities, no influence of splashing was observed (with a reference wind speed U_{10} – i.e. in the upstream undisturbed flow at 10 m height – up to 10 m/s and with drop sizes mainly between 1.0 and 3.0 mm) ([19,20]). From these observations, we can conclude that splashing does not occur for less severe WDR conditions.

Condensation on the gauge collection area can be estimated based on numerical simulations with Heat-Air-Moisture (HAM) transfer models. To provide some indication of this error for this study, a simulation was made for a typical north-west European climate using the HAM-model by Janssen et al. [21]. The Test Reference Year from Essen (Germany) was adopted, for cloudy (rainy) conditions (cloud factor 0.6). The wall assembly behind the gauge area was taken as described in [21]: an insulated, nearly vapour-tight cavity wall facing south-west. The calculated maximum daily value of the condensation volume is 0.15 mm (with 0.3% probability). However, for 90% of the time, it is less than 0.03 mm and for

72% of the time, it is below 0.002 mm. Note that the condensation error will contribute to the cumulative WDR unlike all other WDR errors.

Wind errors are caused by the disturbance of the wind-flow pattern and the raindrop trajectories near the gauge by the presence of the gauge itself (Fig. 10). These errors are expected to be less important for wind directions that are approximately perpendicular to the collection area, given the small wind speed that will exist near the surface. For oblique wind directions, higher wind-speed values will exist near the surface and the influence of the rim of the gauge on the wind-flow pattern and on the raindrop trajectories will become more important. Fig. 10 shows a cross-section with a horizontal plane of two WDR gauges on a wall surface, one with a high rim and one with a low rim. Fig. 10a schematically represents the different wind-flow pattern around the gauges for an oblique wind angle and Fig. 10b shows the raindrop trajectories near the gauges. The gauge with the larger rim causes a larger disturbance of the wind flow and hence of the raindrop trajectories and will therefore catch less WDR.

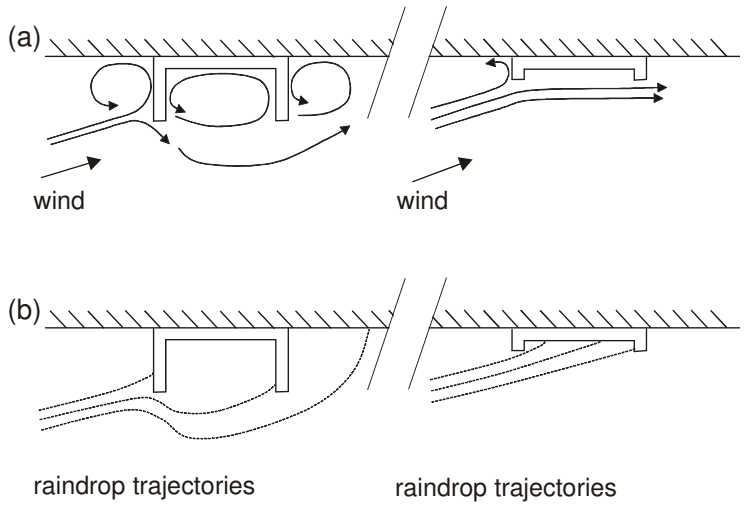

Fig. 10. A cross-section with a horizontal plane of two wind-driven rain gauges on a wall to illustrate the wind error for an oblique wind direction. (a) Wind-flow pattern around the gauges; (b) Raindrop trajectories near the gauges.

5. Guidelines for the design of wind-driven rain gauges

Based on the research work reported in this paper, the following design guidelines for WDR gauges are provided:

1. Limit the amount of adhesion water at the gauge collection area. This can be done by: (1) constructing special WDR gauges (load-cell-suspended or with wiper) or (2) choosing an appropriate gauge material or surface finish to construct traditional WDR gauges. For the latter gauges, plain sheet glass is preferred over PMMA and PVC. PTFE should not be used. When considering the use of other material types or surface finish for the design of traditional WDR gauges, the corresponding amounts of adhesion water should be measured and compared following the procedure described in subsection 3.1.2.
2. Limit the amount of adhesion water at the bottom (horizontal) part of the gauge and in the draining tube. Good drainage from the bottom part to the tube should be provided. The draining tube should be kept as short as possible and the material type should be selected for minimal adhesion water.
3. Evaporative losses from the reservoir can be minimized by exposing only a small water surface to the ambient air, by minimizing the ventilation rate in the reservoir and by regularly adding a few drops of light oil.
4. If possible, direct the collected rainwater towards the inside of the building into reservoirs mounted at the inner wall surface to avoid frost damage to the reservoirs, to reduce the variability in the evaporative losses and to avoid excessive evaporative losses due to heating by solar radiation.
5. Limit the height of the rim of the gauge to reduce the wind errors.

6. Guidelines for selecting accurate wind-driven rain measurement data

Estimating each of the errors associated with WDR measurements is difficult. While three of the five possible error sources, namely adhesion-water evaporation, evaporation from the reservoir and condensation on the collection area can be estimated, the two other sources, splashing and especially wind errors, are not yet sufficiently known. Reliable WDR measurement data for model development and model validation can be obtained by careful selection from WDR measurement databases taking into account the knowledge provided in this paper. The data should be selected for small errors by adhering to the guidelines listed below:

1. Select rain events with large amounts of WDR, hence reducing the relative AW-evaporation error (the AW-evaporation error is especially important for WDR events with small amounts of WDR). The AW-evaporation error should be estimated. This can be done by assuming a worst-case scenario; i.e. complete AW evaporation directly after each interruption of the rainfall by a dry period in the rain event, as described in subsection 3.2.
2. Measure the evaporation from the reservoir and correct the measurements for this error.
3. Select rain events for which splashing errors will be absent or small; i.e. rain events characterised by reference wind-speed values U_{10} lower than 10 m/s and with horizontal rainfall intensities with a small possibility for large drops: $R_h < 20$ mm/h (Best [22]).
4. Although they are generally expected to be small, perform an assessment of the possible condensation error for the meteorological conditions at hand. If these errors can be significant and if they can not easily be eliminated from the data, select rain events for which these errors are small.
5. Select rain events for which the wind direction during rain is approximately perpendicular to the facade under study, hence limiting the wind error.

7. Application

As an example, some WDR measurements that were conducted on the low-rise VLIET test building are presented.

7.1. Measurement set-up

The measurement set-up for wind, rain and WDR at the VLIET test building of the Laboratory of Building Physics, K.U.Leuven, is described in detail in [23]. Here, only the headlines are given. The building consists of two main modules: a sloped-roof module and a flat-roof module. In between the main modules, there is a small terrace module. Fig. 11 shows the north-west and south-west facade of the building and the building dimensions, including the roof overhang length that varies along the length axis of the building. The reference wind speed U_{10} and the reference wind direction are measured at the top of a meteorological mast (10 m height) that is positioned at 20 m distance from the south-west facade, i.e. outside the wind-flow pattern that is disturbed by the presence of the building (when wind is coming from south-west direction). The optimal position of the mast was determined based on CFD analyses [23].

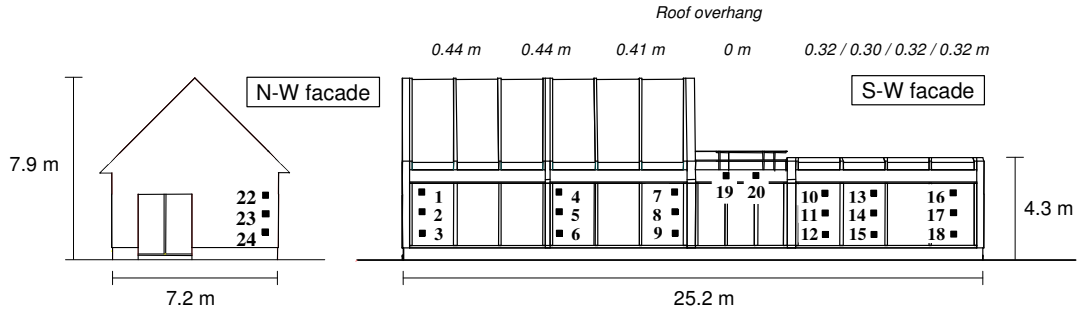

Fig. 11. VLIET test building: north-west and south-west facade. The building dimensions (including roof overhang) and the positions of the wind-driven rain gauges (1-20, 22-24) are indicated.

The horizontal rainfall intensity R_h is measured by a capacitance rain gauge [24] that is installed at ground-level near the meteorological mast. Twenty-three PMMA WDR gauges of the type shown in Fig. 1 are positioned on the south-west and north-west facade. Most of the guidelines mentioned in section 5 were followed. The draining tube is kept as short as possible and it deviates the WDR water to the inside of the building, where it is collected in reservoirs that are fixed at the inner wall surface. The reservoirs are long tubes that are sealed at the top and that are equipped with a pressure sensor to monitor the height of the water level. Pressure equalisation between the air volume in the tube and the ambient air is ensured by a small aperture at the top of the tube. The rim of the gauge is only 10 mm high.

7.2. Measurement results and error estimation

From a database of measurements [23], a number of rain events were selected that are suitable for model development and model validation. One of these is illustrated in Fig. 12. The meteorological data recorded in the period from 25 to 26/02/2002 are shown in Fig. 12a. The horizontal rainfall intensity R_h is light to moderate and the cumulative horizontal rainfall amount for the rain event S_h = 26.7 mm. The wind speed U_{10} varies between 2 and 6 m/s and the wind direction during rain is approximately south-west (225° from north, i.e. perpendicular to the south-west facade). Fig. 12b illustrates the temporal distribution of WDR during this rain event at gauge position 14. During the first 130 minutes of the rain event, no WDR is registered. The roof overhang appears to effectively shelter position 14 during the low wind-speed conditions in the beginning of the rain event. As the wind speed increases and after some delay (gauge collection area first collects adhesion water), WDR is starting to be registered in the reservoir. Fig. 12c shows the variation of the ratio of the accumulated WDR S_{wdr} to the accumulated horizontal rainfall S_h (= 26.7 mm) across the facade for the rain event. In selecting these measurement data, the guidelines in section 6 were followed. The accumulated WDR amounts S_{wdr} are large and the adhesion-water-evaporation error was estimated to be E_{AW} = 5 x 0.10 mm = 0.5 mm (5 interruptions or dry periods and 0.10 mm from Table 2 for the PMMA gauge). The AW evaporation error for the ratio S_{wdr}/S_h at the end of the rain event is $\varepsilon_{AW} = E_{AW}/S_h$ = 0.5 / 26.7 = 0.02, which is a small error. The evaporation from the inside reservoirs was measured (0.05 mm/day) and the measurements were corrected for this. Splashing errors are expected to be negligible given the low wind speed and the low horizontal-rainfall-intensity values. The condensation on the gauge during the rain event is negligible. Wind errors are expected to be small for the gauges at the south-west facade because the wind speed is low and because the wind direction is approximately perpendicular to the south-west facade for this rain event. Note that the WDR measurements by gauges 22-24 are not mentioned here, as the wind error for these measurements will be too high to obtain accurate results.

8. Discussion

All existing semi-empirical models and methods for WDR quantification (the WDR index, the WDR maps and the WDR relationship [1], including the British Standard BS8104 [25] and the European Standard Draft PrEN 13013-3 [26]) are partly or completely based on measurements that were conducted with traditional WDR gauges (i.e. not suspended or wiper-equipped gauges as discussed in section 2). Generally, these models contain parameters that have been fitted to WDR measurements. As the comparative test by Högberg et al. [11] and the present study have shown that WDR measurement errors (underestimations) can be very large, it is possible that the present semi-empirical models and methods underestimate the WDR amount and intensity. Given this possibility, it might be necessary to revise the existing WDR indices, the existing WDR maps and the existing empirical constants in the WDR relationship and in the current standards.

The study in this paper has been limited to plate-type gauges. These gauges are most commonly used in building research, for measurements on buildings as well as for free-field measurements, i.e. measurements of the free WDR without nearby buildings or other obstructions. For other WDR gauges, the same principles apply and similar experiments as in this paper can be conducted.

The first and second guideline in section 5 can be best adhered to by using special WDR gauges, like those illustrated in Fig. 2 and 3. These gauges have very limited amounts of adhesion water and can therefore provide accurate measurements, even for rain events with small WDR amounts. The disadvantage of such gauges however is that their construction and installation is more expensive and more time-consuming. Their use is not (yet) established. Practically all measurements that were conducted in the past were made with traditional WDR gauges. Even today, especially for measurements with a large number of WDR gauges, one generally prefers traditional gauges.

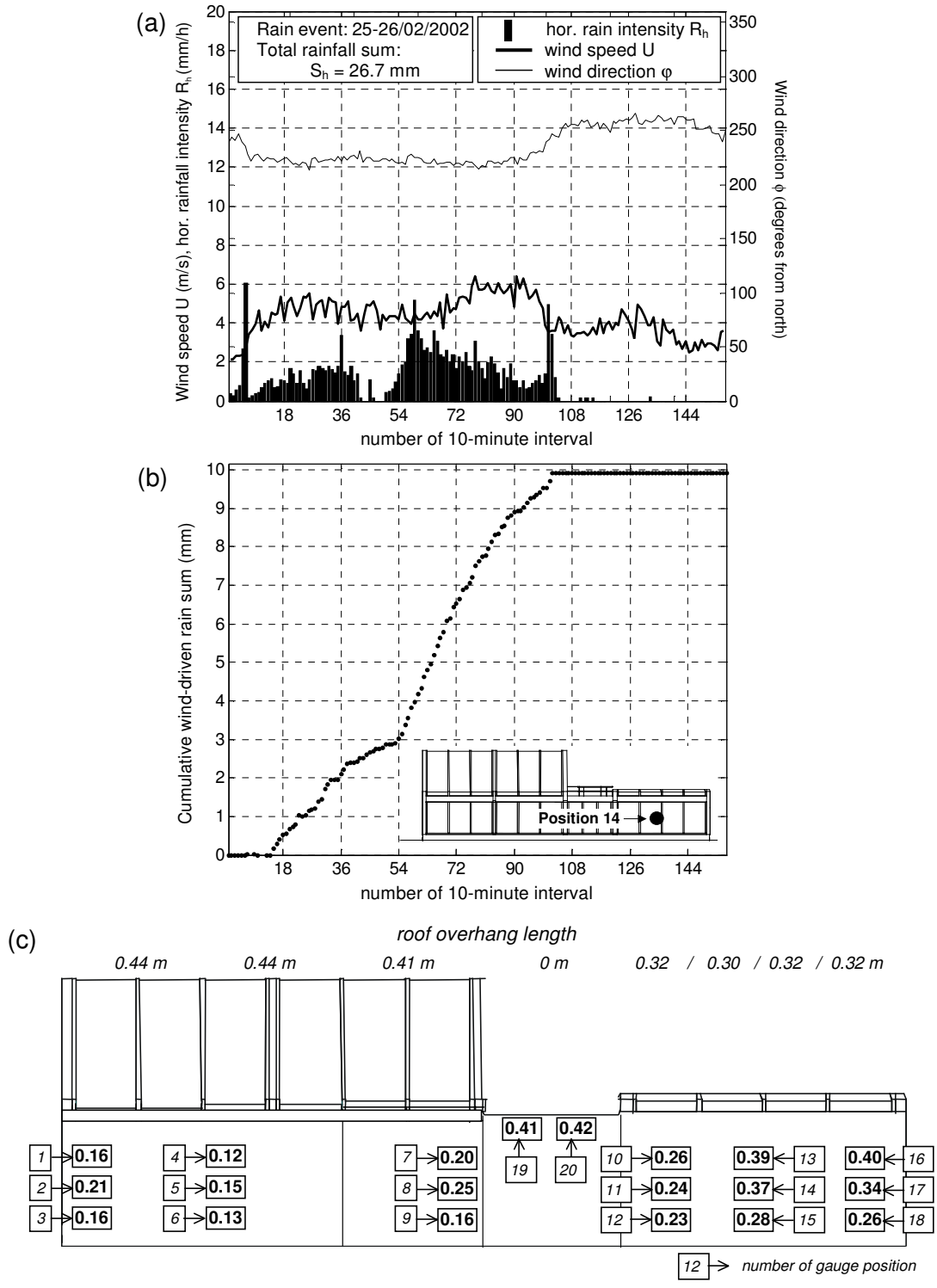

Fig. 12. Measurement results for the rain event during the period 25-26/02/2002. (a) Horizontal rainfall intensity, reference wind speed and wind direction measured during the rain event and averaged on a 10-minute basis. Accumulated horizontal rainfall for the rain event S_h = 26.7 mm. (b) Temporal distribution of the cumulative wind-driven rain amount S_{wdr} during the rain event at position 14 on the south-west facade. (c) Spatial distribution of the ratio S_{wdr}/S_h for the rain event at the south-west facade.

The guidelines for data selection provided in section 6 are strict. It is important to note that following them implies that a large amount of the gathered WDR measurement data can not be used and that measurements for a long period will be needed to obtain a significant number of reliable and useful WDR measurements. The strict character of these guidelines is justified because there are currently no other ways to ensure that the gathered data is accurate.

The study presented in this paper is a first step towards the quantification of the errors associated with WDR measurements. Although the error sources have been identified and one of the most important error sources has been studied in detail, the investigation is not complete. Future research efforts should focus on the following issues:

1. The influence of weathering and soiling of the WDR-gauge collection area on the amount of adhesion water. The experiments presented in this paper were performed for clean material surfaces. A dirty, weathered surface might exhibit a change in surface characteristics which might lead to changes in the amount of adhesion water.
2. The estimation of splashing errors and of wind errors. For the study of wind errors, the use of numerical simulation with CFD is probably the best option.
3. The importance of the different error sources depending on the climate at hand.

9. Conclusions

Knowledge on the accuracy of WDR measurements on buildings is essential in order for these measurements to be used with confidence in WDR studies. The present paper focused on the errors that can be associated with WDR measurements. Guidelines were provided to design WDR gauges and to select accurate and reliable WDR data. The following conclusions are drawn:

- In contrast to the very simple measurement principle, estimating the errors associated with WDR measurements is complicated.
- Five error sources are involved: (1) adhesion-water evaporation, (2) evaporation from the reservoir, (3) splashing of drops from the collection area, (4) condensation on the collection area and (5) wind errors.
- Evaporative loss of adhesion water from the collection area is considered to be one of the most important error sources. It can cause errors up to 100%. Evaporation from the reservoir can be measured and the WDR measurements can be corrected for this error. Estimates of condensation errors can be obtained by a simulation with a Heat-Air-Moisture transfer model. Information about splashing errors and wind errors is limited and further research on these errors is needed. For the investigation of wind errors, the use of CFD is advised.
- Guidelines for the design of WDR gauges and guidelines for the selection of accurate and reliable WDR measurement data from WDR databases have been provided.
- WDR measurements should always be conducted for a sufficiently long period, as only a limited number of measurements will be reliable and will be useful for the interpretation of the WDR exposure of building facades and for model development and model validation.
- The existing semi-empirical models and the current standards are based on WDR measurements with traditional WDR gauges, for which no error estimates were provided. Given the possibility of large measurement errors (underestimations), a revision of these models and standards may be necessary.

Acknowledgements

The first author is a post-doctoral research fellow of the FWO-Flanders (= Research Fund - Flanders; Fonds voor Wetenschappelijk Onderzoek, Vlaanderen). The FWO-Flanders supports and stimulates fundamental research in Flanders. Their contribution is gratefully acknowledged. The authors also want to express their gratitude to Fabien van Mook for the permission to include some of his photographs in this paper and for valuable discussions.

Nomenclature

A	catch area (m²)
A_{AREA}	size of a square area on the collection surface (m²)
d	raindrop diameter (mm)
d_{LIMIT}	limit base diameter of surface-pendent drop for runoff (mm)

d_{SPD}	base diameter of a surface-pendent drop (mm)
d_{TRACE}	base diameter of trace droplet (mm)
E_{AW}	absolute adhesion-water-evaporation error (mm)
e_{AW}	relative adhesion-water-evaporation error ($e_{AW} = E_{AW}/S_{wdr}$) (-)
ε_{AW}	adhesion-water-evaporation error for the ratio S_{wdr}/S_h ($\varepsilon_{AW} = E_{AW}/S_h$) (-)
R_h	horizontal rainfall intensity (mm/h)
R_{wdr}	wind-driven rain intensity (mm/h)
S_h	horizontal rainfall (mm)
s_{AREA}	length/width of a square area on the collection surface (m)
s_{TRACE}	spacing between the trace droplets (m)
S_{wdr}	wind-driven rain (mm)
U_{10}	reference wind speed (m/s)
V_{LIMIT}	limit volume of a surface-pendent drop for runoff (m³)
V_{TRACE}	volume of (surface-pendent) trace droplet (m³)

References

[1] Blocken B, Carmeliet J. A review of wind-driven rain research in building science. Journal of Wind Engineering and Industrial Aerodynamics 2004;92(13): 1079-1130.

[2] Choi ECC. Simulation of wind-driven rain around a building. Journal of Wind Engineering and Industrial Aerodynamics 1993;46&47: 721-729.

[3] Karagiozis A, Hadjisophocleous G, Cao S. Wind-driven rain distributions on two buildings. Journal of Wind Engineering and Industrial Aerodynamics 1997;67&68: 559-572.

[4] Blocken B, Carmeliet J. Spatial and temporal distribution of driving rain on a low-rise building. Wind and Structures 2002;5(5): 441-462.

[5] Van Mook FJR. Driving rain on building envelopes. Ph.D. thesis. Building Physics Group (FAGO), Eindhoven University of Technology, Eindhoven University Press, Eindhoven, The Netherlands; 2002, 198 p.

[6] Segersson D. Numerical quantification of driving rain on buildings, Reports Meteorology and Climatology, No. 103, Swedish Meteorological and Hydrological Institute (SMHI); 2003.

[7] Blocken B, Carmeliet J. The influence of the wind-blocking effect by a building on its wind-driven rain exposure. Journal of Wind Engineering and Industrial Aerodynamics. Revised version submitted. 2005.

[8] Hendry IWL. Comparison between two types of wall rain gauge. Building Research Station, Internal note, SL/IN.1; 1964.

[9] Lacy RE. Driving-rain maps and the onslaught of rain on buildings. RILEM/CIB Symp. on Moisture Problems in Buildings, Rain Penetration, Helsinki; 1965, Vol. 3, paper 3-4

[10] Meert E, Van Ackere G. Dichtheid van gevels en daken (in Dutch). Wetenschappelijk en Technisch Centrum voor het Bouwbedrijf, eindverslag, Brussel; 1977.

[11] Högberg AB, Kragh MK, van Mook, FJR. A comparison of driving rain measurements with different gauges. Proceedings of the 5th Symposium of Building Physics in the Nordic Countries, Gothenburg; 1999, p. 361-368.

[12] Kragh MKK. Microclimatic conditions at the external surface of building envelopes. Ph.D thesis, Department of Buildings and Energy, Technical University of Denmark; 1998.

[13] Van Mook FJR. Description of the measurement set-up for wind and driving rain at the TUE. Report FAGO 98.04.K; 1998.

[14] Van Mook FJR. Measurements of driving rain by a new gauge with a wiper. Report FAGO 98-62.K; 1998.

[15] Couper RR. Factors affecting the production of surface runoff from wind-driven rain. 2nd International CIB/RILEM Symp. on Moisture Problems in Buildings. Rotterdam, The Netherlands; 1974, paper 1.1.1.

[16] Högberg A. Microclimate measurement focused on wind-driven rain striking building surfaces. Proceedings of the 5th Symposium for Building Physics in the Nordic Countries, Gothenburg; 1999, p. 369-376.

[17] Högberg A. Measurement of microclimate near a building surface. Proceedings of the 10th International Symposium for Building Physics and Building Climatology, Dresden, Germany; 1999, p. 649-657.

[18] Högberg A. Microclimate load: transformed weather observations for use in design of durable buildings. Ph.D. thesis, Department of Building Physics, Chalmers University of Technology, Göteborg, Sweden; 2002, 162 p.
[19] Blocken B, van Mook FJR, Högberg A. Full-scale driving rain simulation in the Jules Verne Climatic Wind Tunnel. Training and Mobility of Researchers, Access to Large-Scale Facilities – Access for researchers, Research proposal; 1999, 11 p.
[20] Gandemer J. Final report: Large Scale Facilities, Jules Verne Climatic Wind Tunnel, Contract ERB 4062PL970118; 2001.
[21] Janssen H, Blocken B, Carmeliet J. Conservative modelling of the moisture and heat transfer in building components under atmospheric excitation. International Journal of Heat and Mass Transfer. Submitted. 2005.
[22] Best AC. The size distribution of raindrops. Quarterly Journal of the Royal Meteorological Society 1950;76: 16-36.
[23] Blocken B, Carmeliet J. High-resolution wind-driven-rain measurements on a low-rise building – experimental data for model development and model validation. Journal of Wind Engineering and Industrial Aerodynamics. Revised version submitted. 2005.
[24] Nystuen JA, Proni JR, Black PG, Wilkerson JC. A comparison of automatic rain gauges. Journal of Atmospheric and Oceanic Technology 1996;13(1): 16-36.
[25] British Standards Institution. Code of practice for assessing exposure of walls to wind-driven rain – BS8104, 1992.
[26] CEN. Hygrothermal performance of buildings – Climatic data – Part 3: Calculation of a driving rain index for vertical surfaces from hourly wind and rain data. Draft prEN 13013-3, 1997.

FIGURE CAPTIONS

Fig. 1. Wind-driven rain gauge designed, manufactured and installed at the Laboratory of Building Physics, K.U.Leuven. The gauge is made of PMMA (polymethyl-methacrylate) with a collection area A = 0.2x0.2 m².

Fig. 2. Special wind-driven rain gauge designed to measure adhesion water. The collection plate and the reservoir are suspended from a load cell (figure partly from [5], ©van Mook 2003, reproduced with permission).

Fig. 3. Special wind-driven rain gauge designed to measure adhesion water. The collection area is equipped with an automated wiper (figure partly from [5], ©van Mook 2003, reproduced with permission).

Fig. 4. Measurement set-up for the comparative test of wind-driven rain gauges. (a) The west facade of the TUE main building. The positions of the wind-driven rain gauges that are involved in the test are indicated by the labels "P7", "P5", "P4". (b) Wind-driven rain gauges exposed next to each other. From left to right: the TUD gauge, the CTH gauge, the TUE-I gauge and the TUE-II gauge (figure partly from [5], ©van Mook 2004, reproduced with permission).

Fig. 5. Schematic representation of the numerical model for raindrop adhesion, coagulation and runoff on a vertical surface. (A) and (B) are detail figures of a surface-pendent drop and of two trace droplets, respectively.

Fig. 6. Result of the numerical simulation of drop adhesion, coagulation and runoff on an impervious, smooth, vertical surface. The "cumulative inflicted WDR" is the total amount of rainwater impinging on the surface. The "measured WDR" is the amount that has run off into the reservoir. The curve "adhesion water" indicates the amount of water that is adhered to the surface.

Fig. 7. Photovisual images of sessile water droplets (volume of 1μL) on a horizontal material surface for contact-angle measurements with the optical sessile-drop method. (a) Droplet on a PVC surface with an average contact angle $\gamma_{S,AVG} = 93.5°$. (b) Droplet on an ordinary-sheet-glass surface with an average contact angle $\gamma_{S,AVG} = 24.9°$.

Fig. 8. (a) Contact angle of a sessile drop on a horizontal surface (γ_s). (b) Contact angles of a surface-pendent drop on a vertical surface: advancing (γ_a) and receding (γ_r) contact angles.

Fig. 9. Special wind-driven rain gauge designed to limit splashing losses [18]. The collection area is deeply recessed and is composed of tilted surfaces.

Fig. 10. A cross-section with a horizontal plane of two wind-driven rain gauges on a wall to illustrate the wind error. (a) Wind-flow pattern around the gauges; (b) Raindrop trajectories near the gauges.

Fig. 11. VLIET test building: north-west and south-west facade. The building dimensions (including roof overhang) and the positions of the wind-driven rain gauges (1-20, 22-24) are indicated.

Fig. 12. Measurement results for the rain event during the period 25-26/02/2002. (a) Horizontal rainfall intensity, reference wind speed and wind direction measured during the rain event and averaged on a 10-minute basis. Accumulated horizontal rainfall for the rain event $S_h = 26.7$ mm. (b) Temporal distribution of the cumulative wind-driven rain amount S_{wdr} during the rain event at position 14 on the south-west facade. (c) Spatial distribution of the ratio S_{wdr}/S_h for the rain event at the south-west facade.

Table 1: Plate dimensions and results of the contact-angle and adhesion-water (AW) measurements for six rectangular plates of different materials.

	PVC	PMMA	PTFE	Glass1[a]	Glass2[a]	Glass3[a]
Plate height (m)	0.45	0.45	0.45	0.25	0.30	0.30
Plate width (m)	0.25	0.25	0.25	0.25	0.20	0.20
Contact angle (°)	93.5	100.0	101.9	24.9	14.5	106.6
AW (avg) (mm or L/m²)	0.07	0.06	0.10	0.03	0.03	0.10
AW (stdev) (mm or L/m²)	0.006	0.005	0.007	0.004	0.003	0.009

[a]Glass1 = ordinary glass, Glass2 = with hydrophilic coating, Glass3 = with hydrophobic coating.

Table 2: Adhesion-water (AW) measurements for two wind-driven rain gauges: the PVC gauge and the PMMA gauge of the Laboratory of Building Physics.

	PVC	PMMA
Collection area (m²)	0.3x0.3	0.2x0.2
AW (avg) (L/m²)	0.08	0.10
AW (stdev) (L/m²)	0.011	0.017